J Mater Sci: Mater Electron

Microwave dielectric properties of $BaWO_4$-doped $Ba(Mg_{1/3}Nb_{2/3})O_3$ ceramics

Sen Peng[1,2,*] and Jianming Xu[1]

[1] Provincial Key Laboratory of Informational Service for Rural Area of Southwestern Hunan, Shaoyang University, Shaoyang 422000, China
[2] College of Electrical and Information Engineering, Hunan University, Changsha 410082, China

Received: 20 August 2020
Accepted: 19 October 2020

ABSTRACT

In this paper, $Ba(Mg_{1/3}Nb_{2/3})O_3$ (BMN) ceramics with x (x = 0–9) wt% $BaWO_4$ were synthesized using the conventional solid-state sintering technique. Effects of $BaWO_4$ addition on the microstructure and microwave dielectric properties of BMN ceramics were evaluated. X-ray diffraction (XRD) analysis showed that there were three phases: main crystalline phase $Ba(Mg_{1/3}Nb_{2/3})O_3$ and secondary phases $BaWO_4$ and $Ba_5Nb_4O_{15}$. Meanwhile, the (100) super-lattice reflection peaks shifted to a higher 2θ angle with increasing $BaWO_4$ content. SEM photographs suggested that $BaWO_4$ working as a sintering additive promoted the densification and grain growth. The dielectric properties were examined by Vector network analyzer. The dielectric constant (ε_r) was largely determined by the relative density and phase composition. Meanwhile, the addition of $BaWO_4$ had a positive effect on the $Q \times f$ value, for example the specimen with x = 5 possessed the highest $Q \times f$ value of 111,300 GHz. Optimum microwave dielectric properties (ε_r = 31.7, $Q \times f$ = 111,300 GHz (f = 8 GHz) and τ_f = 0.16 ppm/°C) were obtained for the specimen with x = 5 sintered at 1350 °C for 6 h.

1 Introduction

With the rapid growth of electronic industry, microwave dielectric ceramics have been used as microwave devices such as microwave filters, path antennas and resonators, which have been extensively used in microwave circuits. Therefore, developing an excellent ceramic material has great application value. How to develop a ceramic with applicable dielectric constant, high quality factor and high temperature stability has been becoming a hot research topic in recent years [1–4].

Ceramics with general formula $Ba(B'_{1/3}B''_{2/3})O_3$ (B′ = Mg and Zn, B″ = Nb and Ta), which show unique microwave dielectric properties: high dielectric constant, high quality factor ($Q \times f$) and near zero temperature coefficient of resonant frequency, are widely used as microwave devices for microwave and millimeter wave technologies [5, 6]. Among these materials, $Ba(Mg_{1/3}Nb_{2/3})O_3$ is shown to have the

Address correspondence to E-mail: psen126@hnsyu.edu.cn

https://doi.org/10.1007/s10854-020-04720-w
Published online: 28 October 2020

perovskite structure together with superior microwave properties of the permittivity ε_r = 32, quality factor plus resonant frequency $Q \times f$ = 56,000 GHz, and temperature coefficient of resonant frequency value τ_f = 33 ppm/°C [7]. However, the sintering conditions required to achieve high performance for BMN ceramics are very stringent [7]. The densification sintering temperature of BMN ceramics reach to 1550 °C [7], which is a big obstacle for practical application. In addition, although BMN ceramics possess the high $Q \times f$ value of 56000 GHz, the unacceptably high τ_f value (33 ppm/°C) needs to be adjusted for practical application. In fact, conventional solid-state ceramic route has been used massively, for example, it has been commonly used to realize $Ba(Mg_{1/3}Ta_{2/3})O_3$ ceramics synthesis [8]. However, higher sintering temperature means higher cost, therefore, it's necessary to lower the densification sintering temperature. At present, many methods have been extensively researched, such as changing the sintering process of BMN ceramics and adding the additives into BMN ceramics so as to lower the densification sintering temperature and improve the microwave dielectric properties. Lim [9] used 2 mol% B_2O_3 to decrease the densification sintering temperature of BMN ceramics from 1550 °C to 930 °C, achieving ε_r = 27.5, $Q \times f$ = 8500 GHz and τ_f = + 27 ppm/°C. Sun [10] reported that $Ba([Mg_{1-x}Co_x]_{1/3}Nb_{2/3})O$ (x = 0.8) ceramics could be sintered at 1400 °C, and excellent microwave dielectric properties of ε_r = 31.7, $Q \times f$ = 76,900 GHz and τ_f = + 3.3 ppm/°C were obtained. Shan [11] added 0.25 wt% V_2O_5 to BMN ceramics and decreased the densification sintering temperature to 1350 °C, with good microwave dielectric properties of ε_r = 31.7, $Q \times f$ = 42,100 GHz and τ_f = 22.7 ppm/°C. Wang [12] reported that $Ba_{1-x}Ca_x(Mg_{1/3}Nb_{2/3})O_3$ (x = 0.005) ceramics could be sintered at 1500 °C, and superior microwave dielectric properties (ε_r = 31.64, $Q \times f$ = 74,421 GHz and τ_f = 14.59 ppm/°C) were achieved.

The $BaWO_4$ additive can effectively lower the sintering temperature of the BMN ceramics due to low melting point, and thus could realize the densification sintering of BMN ceramics at a lower temperature. Additional, BMN presents a hexagonal structure, and $BaWO_4$ exhibits a tetragonal structure, therefore, W^{6+} ions substitute Nb^{5+} ions in B″-site to form the solid solutions to some extent. Furthermore, the $BaWO_4$ additive could also modulate the structures and properties of BMN ceramics.

In this study, we tried to sinter BMN ceramics in air by doping a little of $BaWO_4$. The synthesis of the specimens using the conventional solid-state ceramic route was presented, and the replacement of W^{6+} to Nb^{5+} ions was designed in the relatively small range. More significantly, the effect of $BaWO_4$ on phase development, microstructure and microwave dielectric properties of BMN ceramics were researched in detail.

2 Experimental procedures

2.1 Specimen preparation

The specimens were prepared by the conventional solid-state reaction technique. High-purity powders (above 99%) $BaCO_3$, MgO, Nb_2O_5 and $BaWO_4$ were weighed as $Ba(Mg_{1/3}Nb_{2/3})O_3$ + x wt% $BaWO_4$, where x = 0, 1, 3, 5, 7 and 9, then ball-milled in the nylon jar with Al_2O_3 balls and the absolute ethyl alcohol for 18 h, and after drying, these powders were pre-sintered at 1200 °C for 5 h. Then the calcined powders were re-milled for 12 h again and dried in the same way. Later, with 6 wt% acrylic acid solution as binder, the fine powders were pressed into cylindrical samples with 16 mm in diameter and 8 mm in thickness under a pressure of 300 kg/cm^2. Finally, all $BaWO_4$-doped specimens were sintered at 1350 °C for 6 h in air.

2.2 Characterization

X-ray diffraction (DX-1000CSC, Damdong), using CuKα radiation, have been carried out, which identified the phase composition of the specimens. The apparent densities of the specimens were confirmed by the Archimedes method. The microstructures were examined by a scanning electron microscopy(SEM, FEI Inspect F, the United Kingdom). The lattice parameters were calculated through the structure refinement. The cation ordering degree (S) of the specimens is obtained by the equation [13]: $S = \sqrt{\frac{(I_{100}/I_{102})_{obs}}{(I_{100}/I_{102})_{calc}}}$, in which $(I_{100}/I_{102})_{obs}$ is the observed intensities ratio of I_{100}/I_{102} and $(I_{100}/I_{102})_{calc}$ is the calculated values of I_{100}/I_{102}. Excellent microwave dielectric performances were measured at microwave frequencies using a network analyzer (HP83752A) based on the Hakki-Coleman dielectric resonator

method [14]. The τ_f values were determined using the equation: $\tau_f = (f_{t2}-f_{t1})/(f_{t1}\times(t_2-t_1))$, where f_{t1} and f_{t2} are the resonant frequencies at t_1 = 25 °C and t_2 = 85 °C, respectively.

3 Results and discussion

Figure 1 presents the apparent density of the specimens as a function of the sintering temperature and $BaWO_4$ content. Generally, the densification of the ceramics depended heavily on the sintering temperature. For all specimens, the apparent densities first increased to their maximum value at 1350 °C, and then decreased with increasing sintering temperature. The increase of sinterability should be caused by the declination of porosity and grain growth. In contrary, the decrease of the apparent density was ascribed to the deterioration of densification. Associating the above analysis, it was reasonably believed that the optimum sintering temperature of the specimens was about 1350 °C with increasing $BaWO_4$ content. Therefore, all $BaWO_4$-doped specimens were sintered at 1350 °C for 6 h.

X-ray diffraction patterns of BMN ceramics with various $BaWO_4$ contents sintered at 1350 °C are displayed in Fig. 2. According to the crystallographic date base, the main phase of the specimens was indexed to $Ba(Mg_{1/3}Nb_{2/3})O_3$ phase (JCPDS card No. 17-0173) with a hexagonal structure, and the secondary phases of $BaWO_4$ (JCPDS card No. 43-0646; 2.2 wt% with x = 7; 2.5 wt% with x = 9) and $Ba_5Nb_4O_{15}$ (JCPDS card No. 14-0028; 1.9 wt% with x = 7;

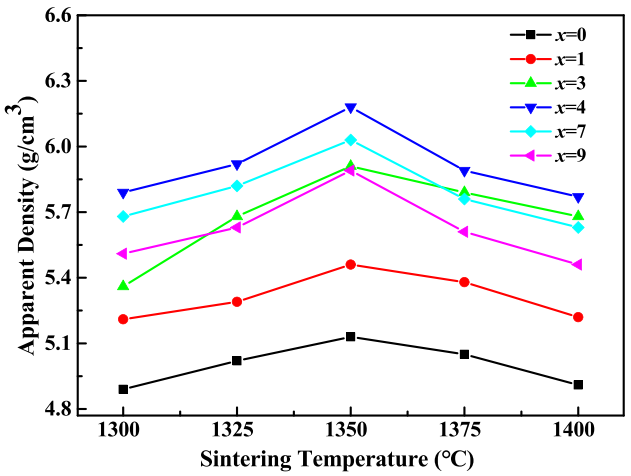

Fig. 1 Apparent density of BMN ceramics with x (x = 0–9) wt% $BaWO_4$ as a function of the sintering temperature

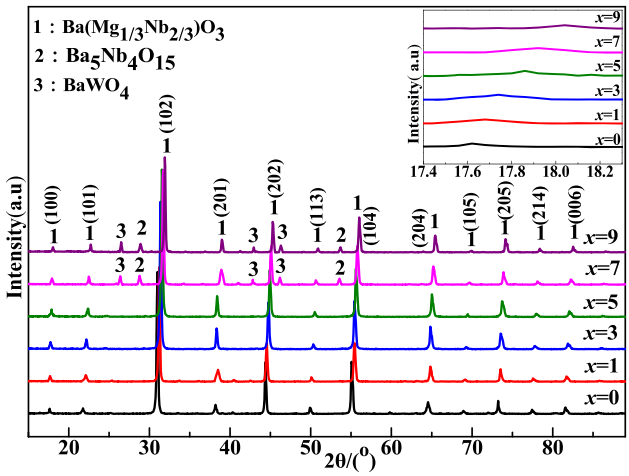

Fig. 2 XRD patterns of BMN ceramics with x (x = 0–9) wt% $BaWO_4$ sintered at 1350 °C for 6 h

2.1 wt% with x = 9) could also be observed when $x \geq 7$, which were not found in other specimens. According to the previous study of BMN-type ceramics [15], when $x \geq 7$, the excessive $BaWO_4$ content in the specimens was favorable to inhibit excessive volatilization of MgO, and the excessive Ba atoms and Nb atoms resulted in the formation of secondary phase $Ba_5Nb_4O_{15}$. In the same addition of $x \geq 7$, the rest of $BaWO_4$ stayed on the grain boundary of the main phase, which existed as liquid state during the high temperature sintering process and as glassy state after cooling [16]. After careful examination of the XRD patterns, it revealed that the (100) reflection peaks, as shown in the inset image in Fig. 2, toward high angle direction with increasing $BaWO_4$ content, which was ascribed to the partial replacement of the smaller W^{6+} (0.6 Å) to Nb^{5+} (0.64 Å) in BMN. Apparently, the valence differences of W^{6+} and Nb^{5+} are smaller than that of W^{6+} and Mg^{2+}. Moreover, considering the ionic radius of Ba^{2+} (1.61 Å), Mg^{2+} (0.72 Å), W^{6+} (0.6 Å) and Nb^{5+} (0.64 Å), it was most likely that W^{6+} ions could only substitute Nb^{5+} ions instead of Mg^{2+} ions in B-site because of the close ionic radius [17, 18], which resulted in the formation of solid solutions.

Table 1 shows the lattice parameters and unit cell volume of BMN ceramics with x (x = 0–9) wt% $BaWO_4$ sintered at 1350 °C for 6 h. As shown in Table 1, the lattice parameters (a, b and c) and unit cell volume decreased accordingly with increasing $BaWO_4$ content. The decrease of lattice parameters and unit cell volume for the specimens was obvious,

Table 1 The lattice parameters and unit cell volume of BMN ceramics with x (x = 0–9) wt% $BaWO_4$ sintered at 1350 °C for 6 h

Specimens	a-axis(Å)	b-axis(Å)	c-axis(Å)	c/a	Unit cell volume(Å^3)
x = 0	5.7673	5.7673	7.0611	1.2243	204.58
x = 1	5.7601	5.7601	7.0532	1.2245	204.21
x = 3	5.7543	5.7543	7.0496	1.2251	203.96
x = 5	5.7426	5.7426	7.0412	1.2261	203.65
x = 7	5.7407	5.7407	7.0311	1.2248	203.47
x = 9	5.7318	5.7318	7.0186	1.2245	203.12

which was attributed to the partial replacement of the smaller W^{6+} (0.6 Å) to Nb^{5+} (0.64 Å) in BMN. Setter and Cross [19] confirmed that the lattice parameters depended heavily on the difference in the average ionic radii in B-site. According to the above analysis, W^{6+} ions could only substitute Nb^{5+} ions in B″-site. The ionic radius of W^{6+} ions (0.6 Å) is smaller than that of Nb^{5+} (0.64 Å) ions in B″-site. Therefore, the substitution of W^{6+} for Nb^{5+} should lead to the decline of the average ionic radii in B-site. As a result, the lattice parameters (a, b and c) decreased accordingly with increasing $BaWO_4$ content. Addition, the unit cell volume decreased from 204.58 Å^3 to 203.12 Å^3 with $BaWO_4$ concentration, thus, it could be inferred that the W^{6+} ion was incorporated into the crystal lattice. It was obvious that the c/a ratio first increased accordingly and then decreased sharply. The most important indicator of the hexagonal distortion caused by the cation ordering was the c/a ratio in the BMN ceramics. It was well known that cation ordering degree and c/a ratio had positive effects on microwave dielectric properties of dielectric ceramics, especially the $Q \times f$ values.

To research the relationship between the $BaWO_4$ amount and the microstructure, the SEM photographs of BMN ceramics doped by x wt% $BaWO_4$ sintered at 1350 °C for 6 h are shown in Fig. 3. It was observed in Fig. 3a that the specimen with x = 0 had an average grain size of about 1.5 μm as well as a lot of residual pores, which indicated the insufficient sintering and low density. From Fig. 3b and c, we could find that the grain growth was improved and the average grain size was approximately from 2 to 5 μm. Meanwhile, the number of the pores decreased significantly, and the densification of these specimens were relatively high. However, there were also many small grains. When x value was further increased to 5 (Fig. 3d), the densification of the specimen increased and the grains were homogeneous, at the same time, their grain boundaries were clear. The grain growth was attributed to the migration and diffusion of ions, which was largely determined by the replacement of W^{6+} to Nb^{5+} ions. Tang [20] verified that the densification process of sintered ceramics by solid-state reaction technique was mainly dependent on the migration and diffusion of ions, and the replacement of W^{6+} to Nb^{5+} ions would promote the migration and diffusion of ions. In this case, the grain growth was promoted accordingly with increasing x value. When x = 7 and 9, the specimens still had dense microstructures, but a few abnormal grains were observed. It was reported that, when the liquid phase exceeded a certain quantity, grain growth was inhibited [21–23]. The abnormal grains might affect the $Q \times f$ value.

To further study the compositions of the abnormal grains mentioned above, the energy dispersive X-ray spectrometer (EDS) for both large and small grains of the specimens with x = 7 and 9 sintered at 1350 C for 6 h (Fig. 3e and f) is shown in Table 2. It could be seen that the small grains (spot A and C) presented Ba : Nb elemental molar ratios of 30.16 : 20.11 and 29.92 : 19.92, respectively, similar to that in $Ba(Mg_{1/3}Nb_{2/3})O_3$. The Ba : Mg : W : Nb elemental molar ratio in the large grains (spot B and D) were approximated 25.38 : 5.83 : 3.01 : 18.13 and 25.25 : 5.61 : 4.12 : 17.81, respectively. Combining with the above XRD analysis, it indicated that the small grains (spot A and C) should be $Ba(Mg_{1/3}Nb_{2/3})O_3$ grains and the large grains (spot B and D) located at the liquid phase. And the EDS analyses revealed that the agglomeration of liquid phase was also Ba-Nb-based phase, however, the elemental molar ratio of W was relatively high. So it could be inferred that there was phase equilibrium among the ternary system $BaWO_4$-liquid phase-$Ba(Mg_{1/3}Nb_{2/3})O_3$ [24]. When $BaWO_4$-doping exceeded a certain quantity, there was evaporation of Nb^{5+} ions, which was ascribed to the replacement of W^{6+} to Nb^{5+} ions in BMN [25]. According to the above XRD analysis, W^{6+} substituted for Nb^{5+} here, while

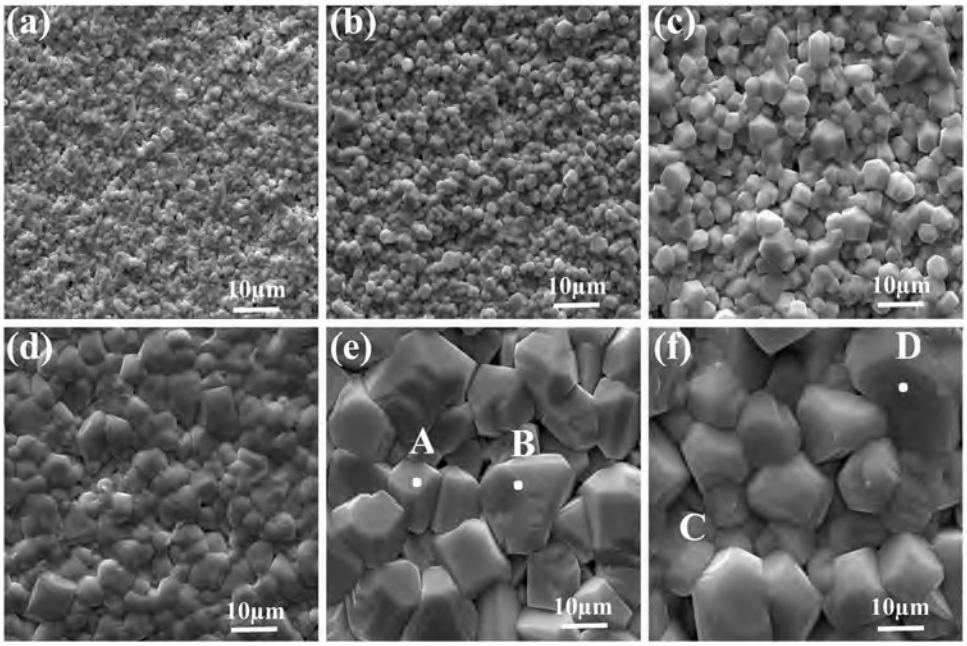

Fig. 3 SEM photographs of BMN ceramics doped by x wt% $BaWO_4$ sintered at 1350 °C for 6 h with **a** $x = 0$, **b** $x = 1$, **c** $x = 3$, **d** $x = 5$, **e** $x = 7$, **f** $x = 9$

Table 2 Energy dispersive X-ray spectrometer (EDS) analysis of the specimens with $x = 7$ and 9

Spot	Mole fraction/(%)				
	Ba	Mg	W	Nb	O
A	30.16	6.22		20.11	43.51
B	25.38	5.83	3.01	18.13	47.65
C	29.92	6.33		19.92	43.83
D	25.25	5.61	4.12	17.81	47.21

excessive $BaWO_4$ could result in the formation of secondary phases $BaWO_4$ and $Ba_5Nb_4O_{15}$. This was demonstrated by the appearance of $BaWO_4$ and $Ba_5Nb_4O_{15}$ peaks with $BaWO_4$ concentration as shown in Fig. 2.

The apparent density and relative density of BMN ceramics with x ($x = 0$–9) wt% $BaWO_4$ sintered at 1350 °C for 6 h are plotted in Fig. 4. It could be seen that the apparent density displayed a similar changing trend compared to the change of relative density. When x value was added from 0 to 5, the densities of the specimens were noticeably increased from 5.13 to 6.18 g/cm^3 with increasing $BaWO_4$ content, and for $x = 5$, there was a peak value for apparent density owing to the migration and diffusion of ions caused by the replacement of W^{6+} to Nb^{5+} ions in BMN. Combining with Figs. 3 and 4, the grain growth was promoted and the densification of the specimens

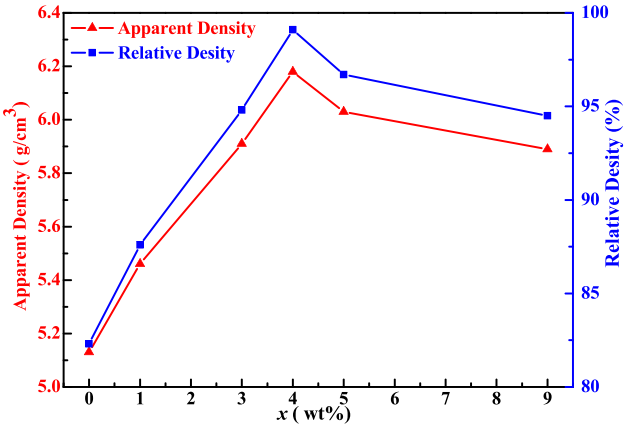

Fig. 4 Apparent density and relative density of BMN ceramics with x ($x = 0$–9) wt% $BaWO_4$ sintered at 1350 °C for 6 h

were gradually increased as increasing $BaWO_4$ content. Thus, W^{6+} substitution promoted the atomic diffusion and mass transfer, in this case, the grain growth was promoted accordingly with increasing x value. When $x \geq 7$, the densities started to decline with increasing $BaWO_4$ content, which was caused by the abnormal grain growth as shown in Fig. 3e–f. Compared with the apparent density, the relative density was considered to be used for the densification of ceramics. As shown in Fig. 4, the relative densities of the specimens with $x = 1$–9 were above 87%, which were related to the dense microstructures observed in Fig. 3. The increase in the relative density with increasing $BaWO_4$ content could be observed

obviously by the SEM photos. A slight decline in the relative density might be correlated with the abnormal grain growth.

Figure 5 presents the $Q \times f$ values and cation ordering degree(S) of BMN ceramics with x (x = 0–9) wt% $BaWO_4$ sintered at 1350 °C for 6 h. Let us first pay attention to the cation ordering degree. When increasing $BaWO_4$ content, the S values initially increased to a peak value and decreased thereafter. Generally, the cation ordering degree was largely determined by the valence difference of the ions in B-site and the ionic radius difference between the B-site ions [16]. That was, the greater the differences in valence and ionic radius, the more easily the ordered structure would form. After the replacement of W^{6+} to Nb^{5+} ions in B″-site of BMN, the valence differences of Mg^{2+} (0.72 Å) and W^{6+} (0.6 Å) were larger than that of Mg^{2+}(0.72 Å) and Nb^{5+} (0.64 Å). Also, the ionic radius differences of Mg^{2+} (0.72 Å) and W^{6+} (0.6 Å) were larger than that of Mg^{2+}(0.72 Å) and Nb^{5+} (0.64 Å). Therefore, the substitution of W^{6+} for Nb^{5+} ions effectively enlarged the valence and ionic radius differences between the B-site ions simultaneously. Thus, the cation ordering degree gradually increased at $x \leq 5$ with $BaWO_4$ concentration. Furthermore, associating with Fig. 2, the decline in S values was due to the surplus $BaWO_4$ addition, which resulted in the formation of secondary phases $BaWO_4$ and $Ba_5Nb_4O_{15}$. As shown in Fig. 5, the variation of the $Q \times f$ values was in accord with the proportion of $BaWO_4$. The $Q \times f$ values first increased to a peak value of 111,300 GHz with x = 5, then it began to decrease with increasing $BaWO_4$ content. According to the above analysis, it was shown that the $Q \times f$ values displayed the similar changing tendency compared to the change of cation ordering degree. And it indicated that the $Q \times f$ values depended heavily on the cation ordering degree. Therefore, the variation of $Q \times f$ values should be consistent with the cation ordering degree. The careful examination of the Fig. 5 shows that the W^{6+} substitution led to the increase of cation ordering degree from 0.806 to 0.953 as well as the $Q \times f$ values from 46,300 GHz to 111,300 GHz. Therefore, the cation ordering degree played an important role in improving $Q \times f$ values in the specimens.

The variation of the dielectric constant (ε_r) as a function of $BaWO_4$ content displays a similar trend as the apparent densities, as shown in Fig. 6. The dielectric constant (ε_r) initially increased quickly from 30.1 to 31.7 with increasing $BaWO_4$ content from x = 0 to 5, and then the ε_r decreased slowly to 30.9 when x was further increased to x = 9. Generally, the dielectric constant was mainly dependent on the relative density and phase composition. As increasing x value, the relative density of the specimens increased sharply, and reached a peak value at x = 5, which was due to the improvement of densification. To an extent, the relative density of ceramics determined the dielectric constant, probably due to the obtaining of the well compact and uniform microstructures at high densities. Meanwhile the phase composition also strongly influenced the dielectric constant. When x was further increased with $x \geq 7$, the dielectric constant showed a decreasing trend, which could be attribute to the formation of abnormal grains and secondary phase $BaWO_4$. Combining with Figs. 2, 3 and 6, the

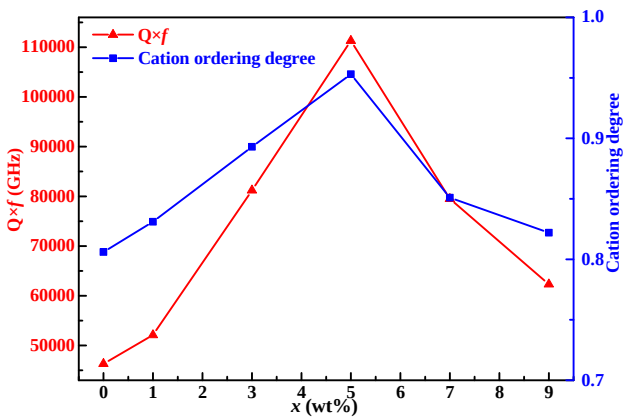

Fig. 5 $Q \times f$ values and cation ordering degree of BMN ceramics with x (x = 0–9) wt% $BaWO_4$ sintered at 1350 °C for 6 h

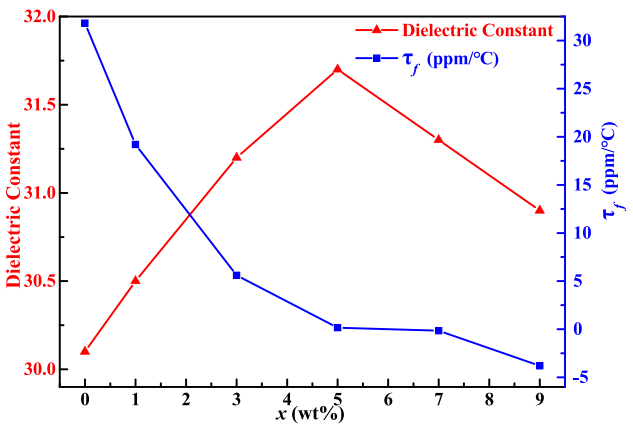

Fig. 6 Dielectric constant (ε_r) and τ_f values of BMN ceramics with x (x = 0–9) wt% $BaWO_4$ sintered at 1350 °C for 6 h

formation of abnormal grains and secondary phase $BaWO_4$ should be responsible for the decrease of the dielectric constant. Moreover, considering the dielectric constant of secondary phases $BaWO_4$ (8.2 [16]) and $Ba_5Nb_4O_{15}$ (39 [26]), and the dielectric constant of $BaWO_4$ (8.2 [16]) was much smaller than that of BMN (32 [7]), thus it was most likely that secondary phase $BaWO_4$ played an important role in decreasing the dielectric constant of the specimens. As shown in Fig. 6, the temperature coefficient of resonant frequency (τ_f) decreased monotonically from + 31.8 ppm/°C to − 3.8 ppm/°C when x was increased from x = 0 to x = 9, and the near-zero τ_f value was + 0.16 ppm/°C with x = 5. Based on the above results, the τ_f values of the specimens dropped quickly when more $BaWO_4$ was added, because $BaWO_4$ phase, with small τ_f value, increased. The τ_f value of the $BaWO_4$ (− 33 ppm/°C [16]) is less than that of BMN (+ 33 ppm/°C [7]), indicating a negative shift of τ_f with $BaWO_4$ concentration. So as presented in Fig. 6, the τ_f values decreased gradually with increasing $BaWO_4$ content.

As shown in Table 3, the specimen with x = 5 could be well sintered at 1350 °C for 6 h and obtained superior microwave dielectric properties: high dielectric constant ε_r = 31.7, high $Q \times f$ = 111,300 GHz, and near-zero temperature coefficient of resonant frequency τ_f = + 0.16 ppm/°C. In addition, These BMN systems were promising for the application of microwave devices such as microwave filter, path antennas and resonators due to their excellent microwave dielectric properties shown in Table 3. The careful examination of the Table 3 shows that the improvement of sintering property and microwave dielectric properties was obvious with the change of the times. The above results indicated that $BaWO_4$ doping not only improved the microwave dielectric properties, but adjusted the temperature coefficient of resonant frequency.

4 Conclusions

The effect of $BaWO_4$ addition on the sintering process and microwave dielectric properties of BMN ceramics were studied by the conventional solid-state ceramic route. The microwave dielectric properties of the specimens were exhibited by XRD, SEM and Vector network analyzer. The results showed that the lattice parameters (a, b and c) and unit cell volume gradually decreased with the $BaWO_4$ concentration; the c/a ratio and the cation ordering degree initially increased to a peak value at x = 5, and then gradually declined with increasing $BaWO_4$ content. SEM photographs suggested that $BaWO_4$ working as a sintering additive promoted the densification and grain growth. As increasing x from 0 to 9, the dielectric constant (ε_r) initially increased quickly from 30.1 to 31.7 with increasing $BaWO_4$ content from x = 0 to 5, and then the ε_r decreased slowly to 30.9 when x was further increased to x = 9, and the $Q \times f$ values first increased from 46,300 GHz to the peak value of 111,300 GHz (x = 5) and decreased to 62,300 GHz thereafter. Meanwhile the temperature coefficient of resonant frequency (τ_f) decreased continuously from 31.8 ppm/°C to -3.8 ppm/°C, and the near-zero τ_f value was + 0.16 ppm/°C with x = 5. At last, BMN ceramics with 5 wt% $BaWO_4$ sintered at 1350 °C for 6 h had a dense microstructure and possessed optimum microwave dielectric properties: ε_r = 31.7, $Q \times f$ = 111,300 GHz (f = 8 GHz) and τ_f = 0.16 ppm/°C. This composition is promising for application in microwave devices such as microwave filters, path antennas and resonators.

Table 3 The microwave dielectric properties of some typical $Ba(Mg_{1/3}Nb_{2/3})O_3$-based ceramics

Year	Ceramics composition	Sintering temperature (°C)	ε_r	Q·f (GHz)	τ_f (ppm/°C)	Reference
1983	$Ba(Mg_{1/3}Nb_{2/3})O_3$	1550	32	56000	33	[7]
1998	$Ba(Mg_{1/3-x}Nb_{2/3})O_3$ (x = 0.02)	1450	32	96000	30	[27]
2004	$Ba(Mg_{1/3}Nb_{2/3})O_3$ + 2 mol% B_2O_3	930	27.5	8500	27	[9]
2007	$Ba(Mg_{1/3}Nb_{2/3})O_3$ + 0.25 wt% V_2O_5	1350	31.7	42100	22.7	[11]
2013	$Ba([Mg_{1-x}Co_x]_{1/3}Nb_{2/3})O_3$ (x = 0.8)	1400	31.7	76900	3.3	[10]
2019	$Ba_{1-x}Ca_x(Mg_{1/3}Nb_{2/3})O_3$ (x = 0.005)	1500	31.64	74421	14.59	[12]
2020	$Ba(Mg_{1/3}Nb_{2/3})O_3$ + 5 wt% $BaWO_4$	1350	31.7	111300	0.16	This work

Acknowledgements

This work was supported by the scientific Research Fund of Hunan Provincial Education Department (Grant No. 18B428).

References

1. H. Li, X.Q. Chen, Q.Y. Xiang, B. Tang, J.W. Lu, Y.H. Zou, S.R. Zhang, Ceram Int. **45**, 14160 (2019)
2. D. Zhou, L.X. Pang, D.W. Wang, I.M. Reaney, J. Mater. Chem. **6**, 9290 (2018)
3. L.X. Pang, D. Zhou, J. Am. Ceram. Soc. **102**, 2278 (2019)
4. D. Zhou, L.X. Pang, D.W. Wang, C. Li, B.B. Jin, I.M. Reaney, J. Mater. Chem. **5**, 10094 (2017)
5. H. Hughes, D.M. Iddles, I.M. Reaney, Appl. Phys. Lett. **79**, 2952 (2001)
6. J.I. Yang, S. Nahm, C.H. Choi, H.J. Lee, H.M. Park, J. Am. Ceram. Soc. **85**, 165 (2002)
7. S. Nomura, Ferroelectrics **49**, 61 (1983)
8. S. Peng, M.Q. Wu, J.M. Xu, T.C. Huang, G.F. Luo, J.K. Yu, J.H. Zhou, J. Mater. Sci.: Mater. Electron. **28**, 3349 (2017)
9. J.B. Lim, J. Son, S. Nahm, W.S. Lee, M.J. Yoo, N.G. Gang, H.J. Lee, Y.S. Kim, Jpn. J. Appl. Phys. **43**, 5388 (2004)
10. T.L. Sun, L. Li, M.M. Mao, X.M. Chen, Int. J. Appl. Ceram. Technol. **10**, E210 (2013)
11. L. Shan, W. Pan, Key Eng. Mater. **336**, 301 (2007)
12. H. Wang, R.L. Fu, H. Liu, J. Fang, G.J. Li, J. Mater. Sci.: Mater. Electron. **30**, 5726 (2019)
13. M.S. Fu, X.Q. Liu, X.M. Chen, Y.W. Zeng, J. Am. Ceram. Soc. **93**, 787 (2010)
14. B.W. Hakki, P.D. Coleman, IEEE Trans. Microwave Theory Tech. **8**, 402 (1960)
15. S. Peng, G.F. Luo, M.Q. Wu, S.Q. Yu, J.M. Xu, T.C. Huang, J.H. Zhou, J. Electron. Mater. **46**, 2172 (2017)
16. S.Z. Jiang, Z.X. Yue, F. Shi, J. Alloys Compd. **646**, 49 (2015)
17. R.D. Shannon, Acta Crystallogr. A. **32**, 751 (1976)
18. B. Tang, Q.Y. Xiang, Z.X. Fang, X. Zhang, Z. Xiong, H. Li, C.L. Yuan, S.R. Zhang, Ceram. Int. **45**, 11484 (2019)
19. N. Setter, L.E. Cross, J. Mater. Sci. **15**, 2478 (1980)
20. B. Tang, Z.X. Fang, Y.X. Li, X. Zhang, S.R. Zhang, J. Mater. Sci.: Mater. Electron. **26**, 6585 (2015)
21. C.L. Huang, K.H. Chiang, C.Y. Huang, Mater. Chem. Phys. **90**, 373 (2005)
22. E.Z. Li, S.X. Duan, S.M. Sun, H. Li, Y.A. Mi, X.H. Zhou, S.R. Zhang, J. Electron. Mater. **42**, 3519 (2013)
23. H.F. Zhou, H. Wang, K.C. Li, H.B. Yang, M.H. Zhang, X. Yao, J. Electron. Mater. **38**, 711 (2009)
24. S.Q. Yu, B. Tang, X. Zhang, S.R. Zhang, X.H. Zhou, J. Am. Ceram. Soc. **95**, 1939 (2012)
25. C.L. Diao, C.H. Wang, N.N. Luo, Z.M. Qi, T. Shao, Y.Y. Wang, J. Lu, Q.C. Wang, X.J. Kuang, L. Fang, F. Shi, X.P. Jing, J. Appl. Phys. **115**, 114103 (2014)
26. C. Vineis, P.K. Davies, T. Negas, S. Bell, Mater. Res. Bull. **31**, 431 (1996)
27. J.H. Paik, S. Nahm, J.D. Bylin, M.H. Kim, H.J. Lee, J. Mater. Sci. Lett. **17**, 1777 (1998)